

# Mapping NH<sub>3</sub> in nearby U/LIRGs using the ngVLA

Junko Ueda,<sup>1</sup> Daisuke Iono,<sup>1,2</sup> Shuro Takano,<sup>3</sup>

<sup>1</sup>National Astronomical Observatory of Japan,

2-21-1 Osawa, Mitaka, Tokyo 181-8588

<sup>2</sup>Department of Astronomy, School of Science, SOKENDAI (The Graduate University for Advanced Studies),

Osawa, Mitaka, Tokyo 181-8588, Japan

<sup>3</sup>Department of Physics, General Studies, College of Engineering, Nihon University,

Tamuramachi, Koriyama, Fukushima 963-8642

## Abstract

The ammonia molecule (NH<sub>3</sub>) is a powerful tracer of the gas kinetic temperature in the interstellar medium, with the main emission lines seen in the 20–30 GHz range (Band 4 of ngVLA). We propose to map the NH<sub>3</sub> line at 300–400 pc resolution in 100 nearby Ultra/Luminous Infrared Galaxies in order to quantify the physical conditions of the star-forming molecular gas in these extreme starburst galaxies. A sensitive and spatially resolved temperature map can provide a better understanding of how galaxy merger event is linked to the nuclear starburst and increased black hole activity. We further comment on the possibility of detecting ammonia from intermediate redshift galaxies using the ngVLA.

Key words: ngVLA<sub>1</sub> — Ammonia<sub>2</sub> — ULIRG<sub>3</sub>

## 1. Introduction

The ammonia molecule (NH<sub>3</sub>) is a powerful tracer of the gas kinetic temperature in the interstellar medium (ISM), with the main emission lines seen in the 20–30 GHz range (Table 1). The quantum energy level is represented by two numbers ( $J, K$ ), where  $J$  is the total angular momentum and  $K$  is the projection along the molecular axis. The spontaneous decay time of the metastable state, that is  $J = K$ , is long ( $\sim 10^9$  sec), and thus the populations between the metastable states are mainly governed by collisions with H<sub>2</sub>. In starless dark clouds, the (1,1) transition is mainly observed. On the other hand, the higher excited transitions, such as (2,2), (3,3), are also observed in star forming molecular clouds including U/LIRG. In environments where the background infrared radiation is significant, the non-metastable states ( $J > K$ ), particularly the (2,1) transition can be observed (e.g. Morris et al. (1973)). Because collision of molecules is the dominant mechanism that dictates the population in the different quantum levels, the relative intensity between different transitions is sensitive to the kinetic temperature of the ISM.

Surveys of the ammonia molecule in the galactic molecular clouds had been carried out since the early days of radio astronomy (Ho & Townes 1983). However, due to the limited sensitivity of the past instruments, most of the extragalactic detections have been limited to a hand-full of bright nearby star forming galaxies (e.g. Mauersberger et al. (2003); Takano et al. (2005); Lebron et al. (2011); Ott et al. (2011); Mangum et al. (2013); Takano et al. (2013); Zschaechner et al. (2016)), starting with a detection of the (1,1) line in IC 342 and NGC 253 (Martin & Ho 1979) using the 100-m telescope at the MPIFR. Despite

Table 1. NH<sub>3</sub> lines ( $J = K$ ) in the 20–30 GHz band

| $(J, K)$ | Frequency [GHz] | $E$ [K]   |
|----------|-----------------|-----------|
| (1,1)    | 23.69449550     | 22.1277   |
| (2,2)    | 23.72263330     | 63.3096   |
| (3,3)    | 23.87012920     | 122.3935  |
| (4,4)    | 24.13941630     | 199.3624  |
| (5,5)    | 24.53298870     | 294.1934  |
| (6,6)    | 25.05602500     | 406.8566  |
| (7,7)    | 25.71518200     | 537.3166  |
| (8,8)    | 26.51898100     | 685.5317  |
| (9,9)    | 27.47794300     | 851.4542  |
| (10,10)  | 28.60473700     | 1035.0308 |

The frequency and energies of the ammonia transitions available in Band 4 of ngVLA (from Splatalogue[1])

the limitations, these studies have demonstrated nicely that the observations of multiple ammonia lines can be a powerful way to quantify the physical properties of the ISM. The "Boltzmann diagram" (the plot of column density vs. rotational energy level) has been used to derive the rotational temperature (and the kinetic temperature assuming the Local Thermal Equilibrium). By observing two or more rotational levels and a linear fit to the column densities, the slope of the corresponding fit yields the rotational temperature. Radiative transfer modeling is used concurrently to derive the physical parameters of the ISM.

The order of magnitude increase in sensitivity offered by the next generation Very Large Array (ngVLA) provides a unique opportunity to investigate the detailed distribution and kinematics of the ammonia molecule, yielding the distribution of the temperature of the ISM which is not possible to map with the current instruments. We propose

<sup>1</sup> <https://splatalogue.online//index.php>

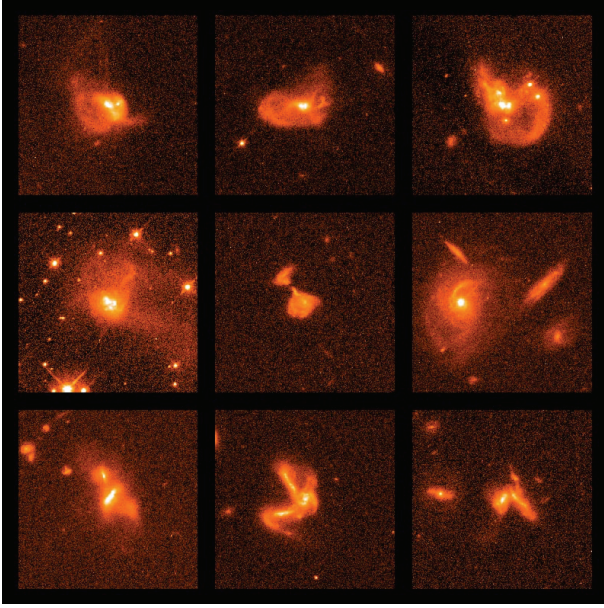


Fig. 1. Optical images of U/LIRGs obtained with the Hubble Space Telescope/Wide Field and Planetary Camera 2[2].

a science case to observe the ammonia molecule in  $\sim 100$  Ultra/Luminous Infrared Galaxies (U/LIRGs) in the local universe, with the main goal to characterise the spatial distribution of the temperature and study its relation to the starburst and Active Galactic Nucleus (AGN) activities traced in optical/IR images. See Wong et al. (2018) for the utility of the ammonia line in nearby galaxies.

## 2. U/LIRG Sample

U/LIRGs are sources which emit the bulk of the emission in the far-infrared (FIR) bands with luminosities of  $10^{11-12} L_{\odot}$ . Morphological studies suggest that interactions and mergers of gas rich galaxies are key dynamical mechanisms which often trigger high degree of starbursts and AGN in the galaxies (Figure 1). The ensemble of dust can be heated to  $\sim 40$  K in part due to the starburst activity (Clements et al. 2018), but note that dust temperature could vary significantly depending on the exact bands used for the SED fit (Mangum et al. 2013).

A wealth of complementary multi-wavelength data exists for 100s of U/LIRGs in the local universe. The Great Observatories All-sky LIRG Survey (GOALS) (Armus et al. 2009) project provides a comprehensive data set using Spitzer, Hubble, Chandra, and GALEX. Some of the sources were followed up in molecular gas using the ALMA telescope (e.g. Ueda et al. (2014)). Out of the sample sources compiled by the GOALS project,  $\sim 130$  sources are observable from the northern hemisphere with good visibility ( $\text{dec} > 10$  deg). The ngVLA science case we

propose in this document is to observe and map multiple transitions of the ammonia line using band 4 of ngVLA toward  $\sim 100$  U/LIRGs in the local universe.

## 3. Feasibility of a U/LIRG Survey

We use the  $\text{NH}_3(1,1)$  line detection toward NGC 253 ( $D_L = 3.44$  Mpc; Mangum et al. (2013)) with the National Radio Astronomy Observatory Green Bank Telescope (GBT) and the properties of Arp 220 ( $D_L = 83.1$  Mpc ( $1'' = 388$  pc)) as a template of ULIRGs for our basis of the feasibility calculation. The target angular resolution is set to  $1''$  to match the resolution of optical/IR images. We scale the  $\text{NH}_3(1,1)$  line strength of NGC 253 to match the predicted line strength of ULIRGs. The peak emission toward NGC 253 is  $T_{\text{mb}} = 72$  mK  $\simeq 300$  mJy beam $^{-1}$  observed with the  $30''$  beam of the GBT ( $30'' \simeq 510$  pc at the distance of NGC 253). Assuming that (1) the strength of the  $\text{NH}_3(1,1)$  line emission per unit area in our target is the same as that of NGC 253 and (2) the uniform distribution of the  $\text{NH}_3(1,1)$  emission within the GBT beam, the observed peak emission toward our target is expected to be  $300 \mu\text{Jy beam}^{-1}$ . According to the ngVLA Performance Estimates, an rms noise (on-source time = 1 hr) is  $24.1 \mu\text{Jy}$  in  $10 \text{ km s}^{-1}$  channel. This would give  $>10$  sigma detection at the peak with a conservative assumption of uniform distribution. The emission will be much stronger in a more realistic case where the filling factor  $< 1$ . According to these estimates, the higher transition lines, even the (9,9) emission which could be 10 times fainter than the (1,1) transition, can be observed with high significance. Lower filling factor is predicted for the transitions with high excitation energies, increasing the chances of detection (and mapping) even further.

## 4. What can be learned?

As a first step, the spatial distribution of the different transitions of ammonia will be compared against each other. In general, higher transition lines trace higher temperature gas, and we expect those lines to be more compact, identifying the regions of elevated star formation activity. The ratio maps (channel maps if sufficient S/N is obtained) along with the help of radiative transfer modeling will allow us to characterize the temperature distribution within each U/LIRG. Lines which are excited at lower and higher energies can be used as tracers of different temperature components of the ISM. For example, as seen in Figure 2, the ratio of the lower transition lines can be a good tracer of the relatively low temperature gas ( $< 50$  K), whereas incorporating the pair of higher transition lines will allow us to probe the warmer component of the gas. One caveat is that multiple temperature components can lie along the same line of sight, in which case one can carefully investigate the distribution in each  $10 \text{ km s}^{-1}$  channel and apply different temperature components for different gas clumps. The ratio of the ortho-lines (i.e. (3,3), (6,6)) can be used as an independent check of the temperature. In addition, detection

<sup>2</sup> Image credits: NASA, Kirk Borne (Raytheon and NASA Goddard Space Flight Center, Greenbelt, Md.), Luis Colina (Instituto de Fisica de Cantabria, Spain), and Howard Bushouse and Ray Lucas (Space Telescope Science Institute, Baltimore, Md).

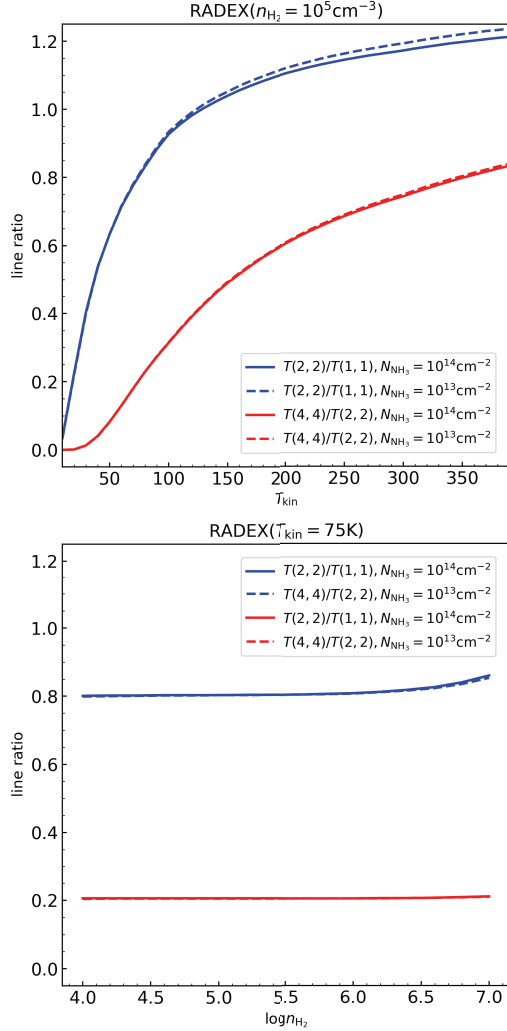


Fig. 2. RADEX calculations of the  $\text{NH}_3$  (2,2)/(1,1) and  $\text{NH}_3$  (4,4)/(2,2) line ratios as functions of the kinetic temperature  $T_{\text{kin}}$  (top) and the  $\text{H}_2$  density  $n_{\text{H}_2}$  (bottom). The line width is fixed to  $10 \text{ km s}^{-1}$ . The line ratios do not mostly change depending on the column density of  $\text{NH}_3$ , so that the solid line ( $N_{\text{NH}_3} = 10^{14} \text{ cm}^{-2}$ ) and dashed line ( $N_{\text{NH}_3} = 10^{13} \text{ cm}^{-2}$ ) overlap.

of both ortho- and para- lines will allow us to derive the spin temperature of ammonia. While ammonia is a good tracer of the temperature, its utility as a density tracer appears relatively insignificant, as seen in the bottom panel of Figure 2. However, when used concurrently with other molecular lines, radiative transfer modeling can allow us to derive the gas density. Absorption may be significant especially at the centers of the U/LIRGs, in which case the temperature of the intervening molecular clouds will be derived. Finally, the temperature map will be compared with maps obtained at similar angular resolution through the archival GOALS data and obtained at the existing facilities such as ALMA, Subaru, etc.

We note that the lines which can be detected in the Band 4 of ngVLA are not limited to the ammonia

Table 2. Notable Molecular Lines in the 20–30 GHz band

| Molecule                              | Frequency [GHz] |
|---------------------------------------|-----------------|
| $\text{HC}_5\text{N}$ ( $J = 8-7$ )   | 21.301252       |
| $\text{CCS}$ ( $J_N = 2_1-1_0$ )      | 22.344033       |
| $\text{HC}_5\text{N}$ ( $J = 9-8$ )   | 23.963910       |
| $\text{HC}_5\text{N}$ ( $J = 10-9$ )  | 26.626547       |
| $\text{HC}_3\text{N}$ ( $J = 3-2$ )   | 27.294327       |
| $\text{HC}_5\text{N}$ ( $J = 11-10$ ) | 29.289159       |

Molecules with  $T_a^* > 1 \text{ K}$  in TMC-1 (Kaifu et al. 2004).

molecule, and others such as carbon-chain molecules (e.g.,  $\text{CCS}$ ,  $\text{HC}_3\text{N}$ , and  $\text{HC}_5\text{N}$ ; see Table 2 for details) can fall into the same IF band coverage. There have been efforts to detect these molecules in nearby galaxies, mainly in millimeter band (e.g., Costagliola et al. 2015). The detection of  $\text{HC}_3\text{N}$  and  $\text{HC}_5\text{N}$  suggests an early, embedded stage of massive star formation (e.g., Rathborne et al. 2008, Taniguchi et al. 2018). The  $\text{NH}_3/\text{CCS}$  ratio has been used as an indicator of chemical evolutionary stage of dark cloud cores in the Galaxy (Suzuki et al. 1992; Hirota et al. 2009). It is possible that utilizing multi-line data offer clues for the starburst phases.

## 5. Redshifted ammonia to trace the cosmic evolution of the physical condition of the ISM

The cosmic history of star formation rate is quantified and reasonably well constrained up to redshifts 2–4, and it is anticipated that ngVLA will be able to measure the history of the gas density up to redshift 4 using the CO (1–0) line as a probe of  $\text{H}_2$  molecule (Decarli et al. 2018). A detailed quantification of the gas temperature evolution across the history of the universe will be a highly complementary probe of the evolution of the physical conditions of the global ISM as a function of cosmic time. The (1,1) ammonia line from galaxies at  $z > 6$  is redshifted to Band 1–2 of ngVLA. The ammonia line, up to the (10,10) transition, has been detected in absorption from lensed sources (e.g. PKS1830-211 ( $z=0.9$ ): Henkel et al. 2008), but studies in the literature are limited and a systematic survey of the ammonia line both in absorption and emission will be an interesting way to utilize the superb sensitivities offered by the ngVLA.

## 6. Summary

The ngVLA will allow us to observe and map the ammonia molecule ( $\text{NH}_3$ ) in 100s of local U/LIRGs at unprecedented quality. The spatially resolved temperature maps will provide us with better understanding of how galaxy merger event is linked to the nuclear starburst and increased black hole activity. Other important molecules will be observed simultaneously in the same band, allowing us to probe the phase of the starburst activities in these merger induced U/LIRGs.

## References

- Armus et al. 2009, *PASP*, 121, 559  
Clements et al. 2018, *MNRAS*, 275, 2097  
Costagliola et al. 2015, *A&A*, 582A, 91  
Decarli et al. 2018, *ASPC*, 517, 581  
Henkel et al. 2008, *A&A*, 485, 451  
Hirota et al. 2009, *ApJ*, 699, 585  
Ho & Townes 1983, *ARA&A*, 21, 239  
Kaifu et al. 2004, *PASJ*, 56, 69  
Lebron et al. 2011, *A&A*, 534, A12  
Mangum et al. 2013, *ApJ*, 779, 33  
Mauersberger et al. 2003, *A&A*, 403, 561  
Martin & Ho 1979, *A&A*, 74, L7  
Morris et al. 1973, *ApJ*, 186, 501  
Ott et al. 2011, *ApJ*, 742, 95  
Rathborne et al. 2008, *ApJS*, 174, 396  
Suzuki et al. 1992, *ApJ*, 392, 551  
Takano et al. 2013, *A&A*, 552, A34  
Takano et al. 2005, *PASJ*, 57, 549  
Taniguchi et al. 2018, *ApJ*, 866, 32  
Ueda et al. 2014, *ApJS*, 214, 1  
Van der Tak et al. 2007, *A&A*, 468, 627  
Wong et al. 2018, *ASPC*, 517, 517  
Zschaechner et al. 2016, *ApJ*, 833, 41